Grain Growth Behaviors in a Friction-Stir-Welded ZK60 Magnesium Alloy

S. Mironov[1,2], Y. Motohashi[1] and R. Kaibyshev[2]

[1]*Research Center for Superplasticity, Faculty of Engineering, Ibaraki University, Hitachi 316-8511, Japan*
[2]*Institute for Metals Superplasticity Problems, Russian Academy of Sciences, 39 Khalturin Str., Ufa, 450001, Russia*

Grain growth during annealing of a friction-stir-welded (FSWed) ZK60 magnesium alloy has been investigated. We have found that (1) thermal stability exhibited in different parts of stirred zone (SZ) was very different, (2) grain growth was fairly abnormal, and (3) grain growth was directional and shapes of developed grains resembled flow patterns inherent to FSWed structure. We have shown that all peculiarities of the grain growth behaviors can be explained in terms of heterogeneous distribution of second phase particles resulted from FSW.
[doi:10.2320/matertrans.MRA2007040]

Keywords: *friction stir welding, abnormal grain growth, magnesium alloy*

1. Introduction

Friction Stir Welding (FSW)[1)] is a promising technique, since it can be used for a solid state joining of many metals and alloys as well as for microstructure refinement; it is now called Friction Stir Processing, FSP. It will be briefly described as follows. A rotating tool is inserted into work pieces to be joined or into a monolithic work piece in case of FSP, and then the tool is moved along the line or curve. During the processing, the material is subjected to a local severe plastic deformation at high temperatures induced by the rotating tool.

The FSW has a number of advantages in comparison with many other methods for the structure refinement. Simplicity and high productivity make this technique very promising for the improvement of superplastic properties of sheet metals. In this regard, the evaluation of thermal stability of the FSW-induced structure must be very important.

According to recent studies, abnormal grain growth (secondary recrystallization) frequently occurs in friction-stir-welded (FSWed) materials.[2–8)] Grain coarsening often initiates at peripheral regions around stirred zone (SZ) of FSWed material,[2,3,5)] and the size of abnormal coarse grains can vary significantly across SZ.[2,6)] Development of these grains was heavily influenced by onion rings structure[2–4,6)] and the growth front was macroscopically uniform though it had some fluctuation in microscopic point of view.[2,3,5)] Low angle boundaries and even small grains were observed within abnormal coarse grains.[2)]

Secondary recrystallization may deteriorate superplastic properties or it may prevent its occurrence. However, clear understanding of this phenomenon is still on its way. The abnormal grain growth in FSWed materials has often been described in terms of Humphreys' theory of stability and growth of cellular microstructures[9,10)] and is usually attributed to the decrease in particles' pinning force due to their partial dissolution.[2–6)]

Up to date, most investigations relating to the grain growth in FSWed materials have been focused on aluminum alloys. Data for other metals, such as magnesium alloys, are required for further progress of the FSW process. In this regard, the present work aims to carry out a detailed study of the grain growth behaviors in a FSWed ZK60 magnesium alloy.

2. Experimental Procedure

The material used was an extruded commercial ZK60 magnesium alloy with the standard chemical composition: Zn 4.8-6.2, Zr 0.5-0.8, Cu $\leq$ 0.03, Ni $\leq$ 0.005 and balance Mg (all in mass%). Strips of $125 \times 50 \times 3\,mm^3$ were cut off from the extruded bar; their longitudinal axis was perpendicular to the extrusion direction. The strips were mechanically polished and then butt joined in pairs along $125 \times 3\,mm^2$ surfaces by a single FSW pass. The welding tool was made from carbon tool steel, SKH9, and consisted of a shoulder having diameter of 14 mm and of a M6 cylindrical pin with 2.8 mm in length. The tool was tilted by 3° from strip normal, such that the rear of the tool was lower than the front and had a shoulder plunge depth of 0.1 mm below the strip surface. The FSW was carried out at tool rotation speed (N) of 600 rpm and at travelling speed (V) of 100 mm/min.

FSWed strips were sectioned along a transversal plane (cross-section). Obtained samples were heat treated at different temperatures in the range of 100 to 450°C for one hour in an air muffle furnace. For inhibition of oxidation during annealing, the samples were imbedded in a container with Al_2O_3 powder. Temperature was controlled by a chromel-alumel thermocouple attached to the samples. The time-temperature plots corresponding to some samples are shown in Fig. 1. As can be seen, the temperatures reached to required levels within the first 15 to 20 minutes during heating and then their deviations did not exceed ±1°C. All samples were water quenched after the heat treatment.

Surfaces of the samples, corresponding to the transversal section of joints, were mechanically ground with water abrasive paper, bath-polished with 1 μm diamond and chemically etched in the solution of 4.2 g picric acid + 65.8 ml ethanol + 10 ml acetic acid + 10 ml distilled water. After etching, they were washed sequentially in ethanol and methanol.

Microstructural observations were made in and around the SZ region only and were performed with an Olympus BX60 optical microscope (OM) and a JSM-5310 scanning electron microscope (SEM). Surface area of second-phase particles per unit volume of material, $\sum S$ (specific surface area), was measured by linear intercept method.[11)] Chemical composi-

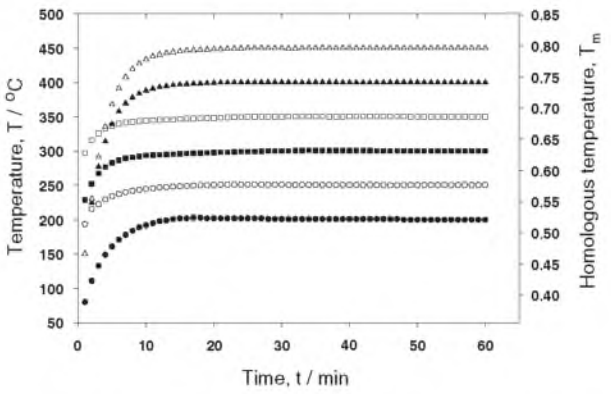

Fig. 1 Time-temperature histories of some samples during heat treatments.

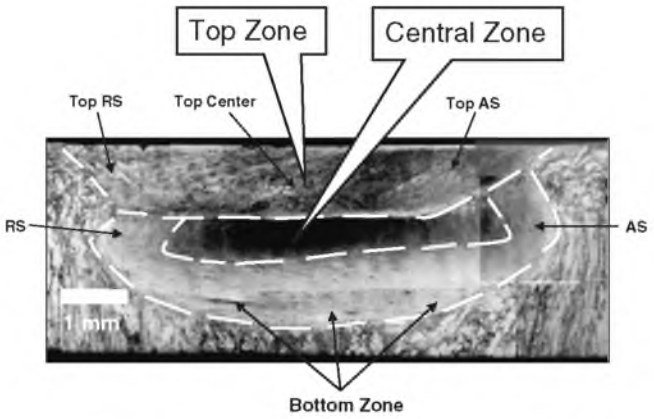

Fig. 2 Macrograph of SZ in as-FSWed state showing various microstructural regions. **Note**: Nugget zone consists of Central and Bottom zones.

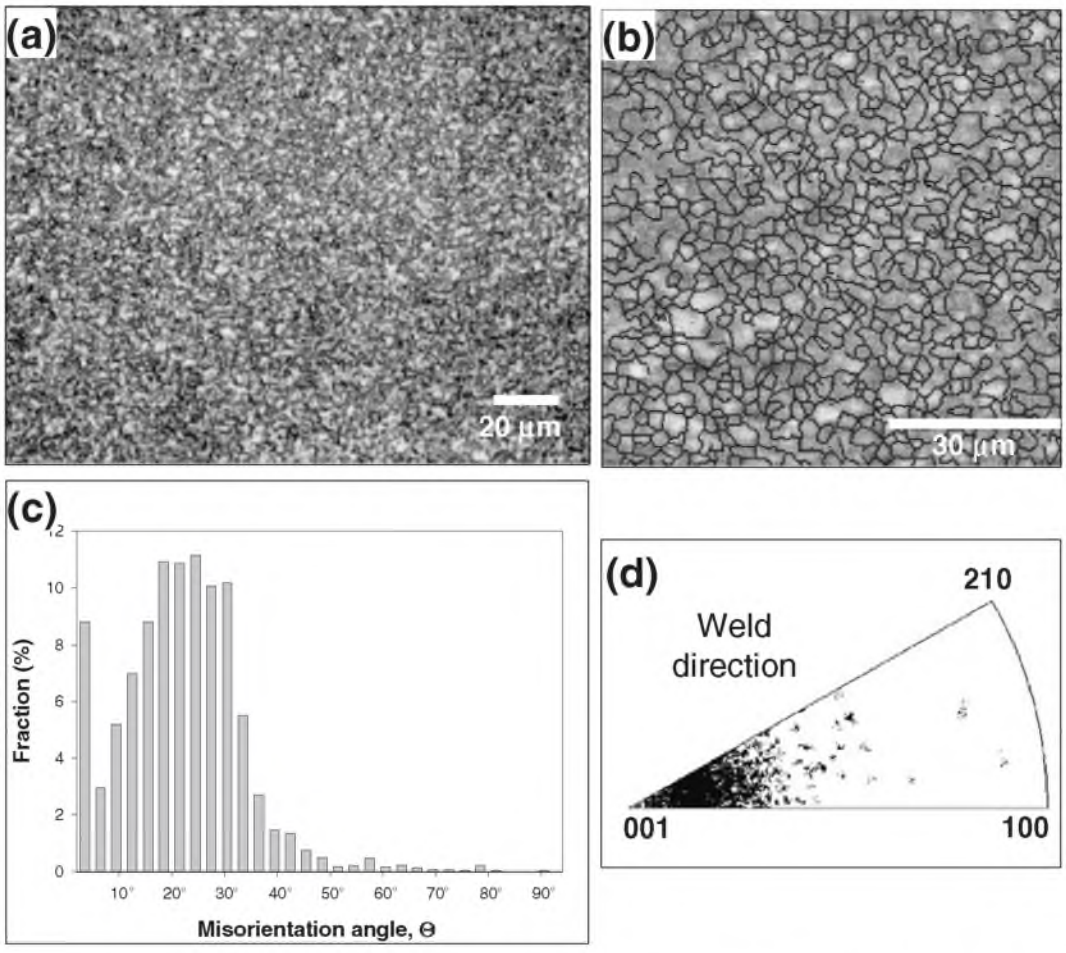

Fig. 3 Typical structure of central region of SZ in as-FSWed state: (a) low magnification image, (b) EBSD-map (high and low boundaries are shown as dark and light lines), (c) boundary misorientation distribution, (d) inverse pole figure for weld direction.

tion of the particles was examined with a Hitachi S-3000N SEM operating at 10 kV and equipped with a Genesis energy-dispersive X-ray spectrometer system. Electron backscatter diffraction (EBSD) orientation maps were obtained using a Hitachi 3500A field emission gun SEM (FEGSEM) equipped with TSL OIM™ EBSD system.

3. Results

3.1 Structure in as-FSWed (initial) state

A macrograph of SZ in as-FSWed state is shown in Fig. 2. As is clearly seen, three macro-scale zones can be discerned: Top, Central, and Nugget; in addition, the microstructure

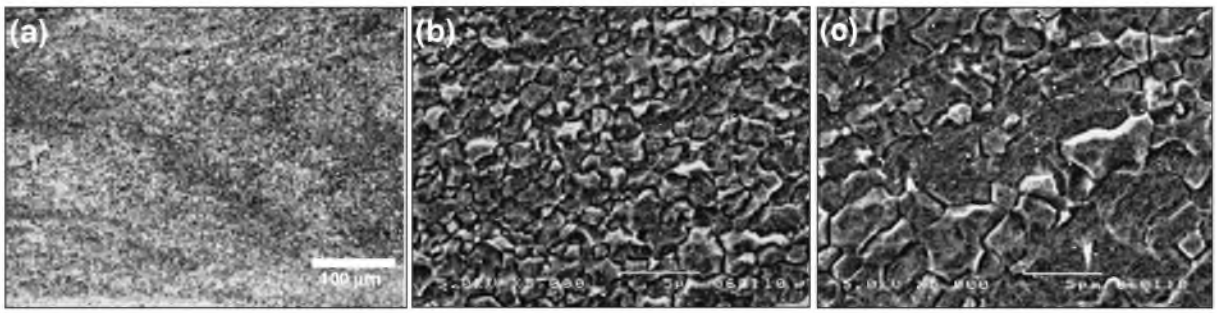

Fig. 4 An example of typical structures of Top zone in as-FSWed state: (a) banded microstructure, (b) high density of particles within fine-grained band, (c) reduced density of particles within coarse-grained band.

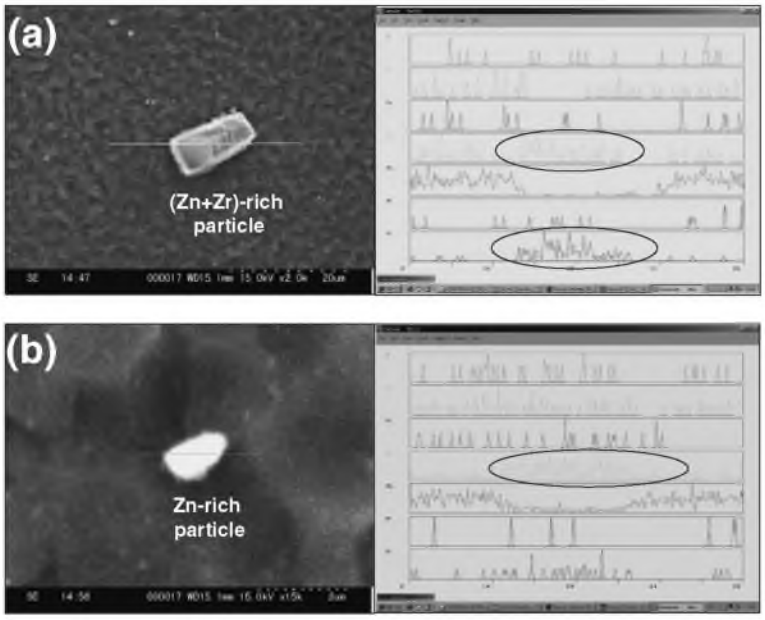

Fig. 5 EDX line scans of particles in central region of SZ in as-FSWed state: (a) coarse particle, (b) middle particle. See text for details.

varies also within these zones from advancing side (AS) to retreating side (RS).

The very specific meso-scale structural features were revealed in Top and Nugget zones; according to Li *et al*,[12] they were interpreted as flow patterns. They were most obvious in Top zone and had a vortex-like shape, twisted from the border between Top and Nugget zones to surface of the sample. Besides, the small vortexes with the strongest optical contrast were found in Top RS and Top Center, which suggested the occurrence of especially complex plastic flow in these regions. The flow patterns in Nugget zone emerged by concentric ellipses extended from Centre to the SZ borders. They are usually referred to as onion rings.[13]

Microstructure of Central zone is given in Fig. 3. The microstructure is homogeneous in an optical scale (Fig. 3(a)) and is comprised of equiaxed fine grains, containing mainly high-angle boundaries (see Fig. 3(b) and (c)). Figure 3(d) indicates that the grains are preferentially oriented such that ⟨001⟩ corresponds to or is close to the weld direction.

Microstructures of Top and Nugget zones are found to be broadly similar to each other and, for simplicity, a typical micrograph taken only from Top zone is shown in Fig. 4. As is seen, the microstructure exhibits two discernible alternating bands and there is a well-defined band-to-band variation in grain size. These bands correlate with the flow patterns spacing and of particular interest is the observation that the fine-grained bands contain a higher density of secondary particles than the coarse-grained ones (see Fig. 4(b) and (c)). Therefore, the typical microstructure in Top and Nugget zones indicates the presence of periodic meso-scale variations in (1) size of equiaxed grains and (2) concentration of second phase particles that correlated with the flow patterns spacing.

Qualitative EDX-analysis is given in Fig. 5. As is seen, coarse particles (Fig. 5(a)) consist mainly of Zn and Zr, whereas middle particles (Fig. 5(b)) are Zn-rich particles.

Table 1 indicates the summarized macro-scale distribution of specific surface area of particles, $\sum S$, within SZ. Some general trends can be derived from the table: (1) $\sum S$ value is lower in the periphery of SZ (Top zone and Bottom) as compared with that in the central part and (2) $\sum S$ value decreases from AS to RS.

3.2 Structure after heat treatment at 100–200°C (0.41–0.52 T_m)

The heat treatments at 100-150°C did not lead to

Table 1 Summarized specific surface area of particles in different regions of Stirred Zone.

	Region of a sample						
	Top AS	Top Center	Top RS	AS	Center	RS	Bottom
Summarized specific surface area of particles, $\sum S$, μm^{-1}	0.17	0.11	0.12	0.42	0.34	0.31	0.20

noticeable changes in structure, while annealing at 200°C increased the density of coarse and middle particles precipitated at grain boundaries.

3.3 Structure after heat treatment at 250–350°C (0.58–0.69 T_m)

Structures evolved in SZ after the heat treatments at 250°C, 300°C and 350°C are shown in Fig. 6 and 7. A common feature, all these structures have, is the appearance of abnormal coarse grains against the initial fine-grained structure (Fig. 2).

Grain growth began at the periphery of the SZ (Top Zone in the first and Bottom in the second) and developed most rapidly in Top RS (Fig. 6(a) and (b)). After the heat treatment at 350°C, abnormal coarse grains nucleated also in RS and (locally) in Central zone and in AS. The best thermal stability was exhibited with the microstructures in Central zone and AS (Fig. 6). Grain shape and grain size of abnormal coarse grains varied significantly across SZ. As is seen in Fig. 6(b) and (c), the shape of grains typically resembles the flow patterns inherent to FSWed structure, meanwhile the coarsest and irregular-shaped grains are developed in the RS and Central zone.

Although boundaries among the abnormal coarse grains were aligned with the flow patterns in meso-scale, growth front was jagged in micro-scale (see Fig. 7(a)). As a result, actual shape of some grains was frequently very complex (Fig. 7(b)). Subboundaries (Fig. 7(c)) and small grains (Fig. 7(a), selected region) were observed within the abnormal coarse grains.

In addition to the abnormal coarse grains and to the stagnated initial ones, the structure exhibited grains of intermediate sizes (Fig. 7(d)). Of particular interest is the observation that these grown grains were frequently grouped in bands aligned with the flow patterns (Fig. 7(e)). Within these bands, grain size varied arbitrary and grains with very different sizes were often neighbouring with each other (Fig. 7(d)). Usually, the smaller grains were equiaxed and the coarser ones were elongated.

The heat treatments at 300°C and 350°C reduced the density of coarse and middle particles to approximately as-FSWed level. The particles were still far from uniform distribution and have been found to be concentrated in bands aligned with the flow patterns (Fig. 7(f)). In addition, particles density within remnants of initial structure was higher than that in the transformed regions. Particles concentrated mainly at grain boundaries, meanwhile, they were found also within the abnormal coarse grains.

3.4 Structure after heat treatment at 400–450°C (0.74–0.80 T_m)

Structures evolved in SZ after the heat treatments at 400°C and 450°C are given in Fig. 8 and 9. Their common feature is the dominance of the abnormal coarse grains (Fig. 8).

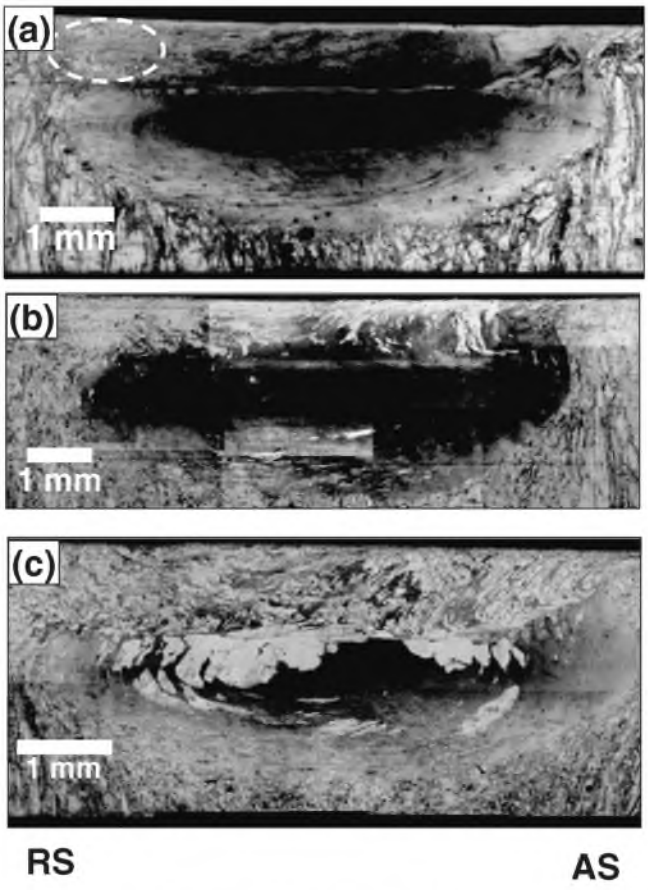

Fig. 6 Macrographs of SZ after heat treatments at 250°C (a), 300°C (b), and 350°C (c). **Note**: Selected (circled) region in Fig. 6a corresponds to the position where abnormal grain growth started at the earliest.

The size of the abnormal coarse grains varied across SZ. As is seen in Fig. 8(a) and (b), the grain size decreases from AS to RS and the grains in the peripheral parts (Top zone and Bottom) are noticeably smaller than the ones in the centre; the coarsest grains are located in Central zone and AS and the smallest one in Top RS. Shape of grains resembled the flow patterns in almost all parts of SZ, except for Central zone, where structure consisted of irregular-shaped single grain (Fig. 8).

Boundaries of the abnormal coarse grains were corrugated and smaller grains were observed in the grain interiors (Fig. 9(a)). The small 'islands' of original structure survived only locally and grain size change in these untransformed regions was negligible as compared to the as-FSWed state (Fig. 9(b)).

Volume fraction of all types of the particles (i.e., coarse, middle and fine particles) increased significantly. Their

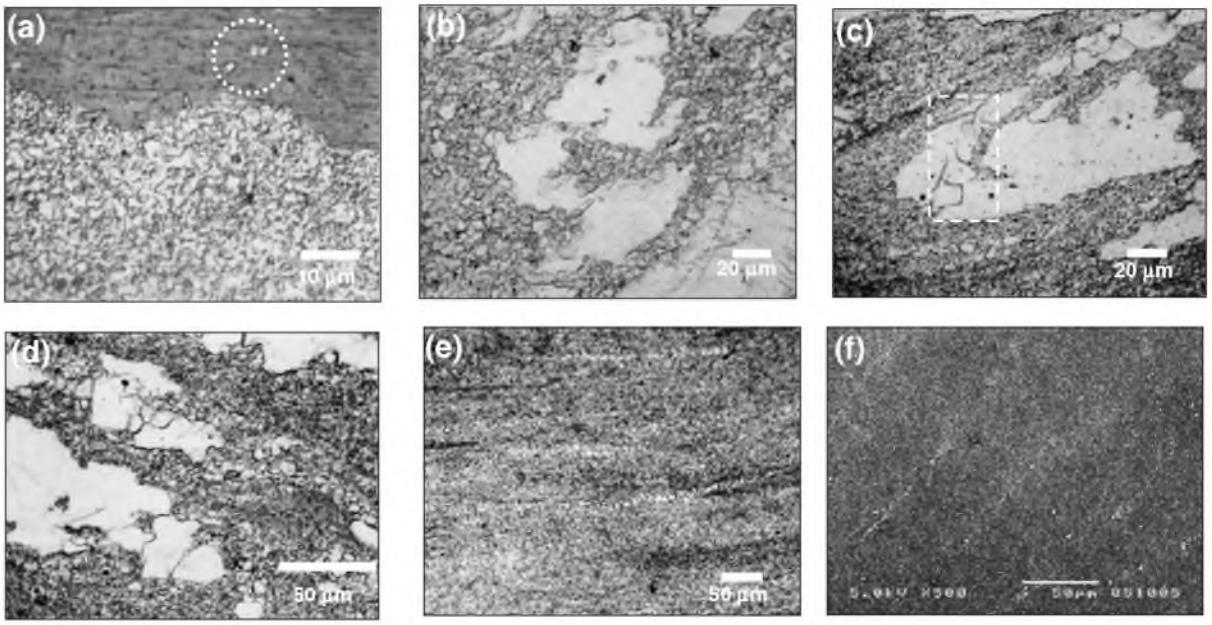

Fig. 7 Features of microstructures after heat treatments at 250°C to 350°C: (a) a jagged boundary of abnormal coarse grain, (b) complex shape of the abnormal coarse grains, (c) subboundaries within the abnormal coarse grain (in selected region), (d) selective grain growth along flow patterns, (e) bands of slightly grown grains, (f) alignment of particles with flow patterns.

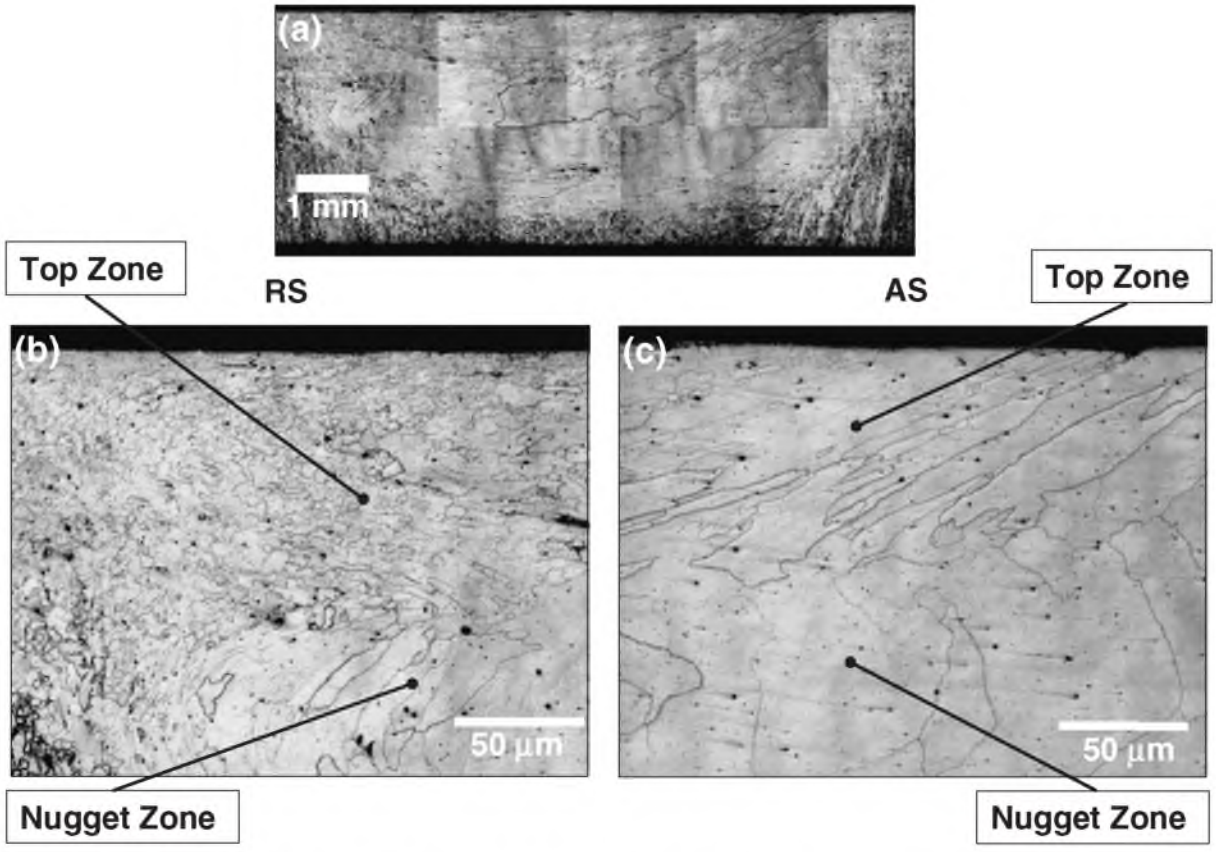

Fig. 8 Structures in SZ after heat treatment at 450°C at low magnifications: (a) macrograph, (b) RS, (c) AS.

spatial distribution was still heterogeneous: (1) the bands of the particles aligned with the flow patterns were observed within the abnormal coarse grains (Fig. 9(c)), and (2) the 'islands' of the survived initial structure were characterized by a higher local density of the particles (Fig. 9(d)).

4. Discussion

As it follows from our experimental results, annealing response the microstructure developed in the FSWed ZK60 magnesium alloy includes particles precipitation at temper-

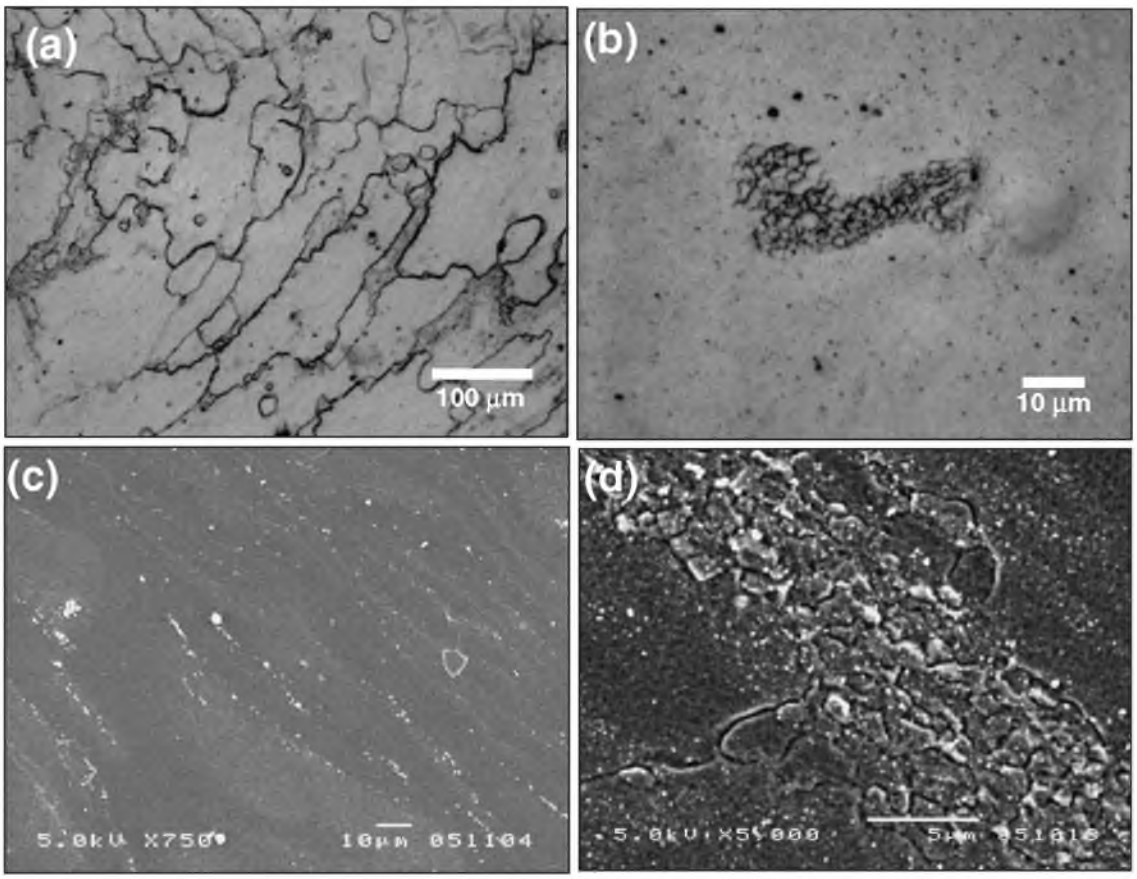

Fig. 9 Microstructures in SZ after heat treatments at 400-450°C: abnormal coarse grains (a), 'island' of survived initial structure (b), alignment of particles with flow patters (c), and high density of particles within the survived 'island' of initial structure (d).

atures ranging from 200 to 250°C and from 400 to 450°C and grain growth at temperatures above 200°C. Any traces of primary recrystallization have not been found.

4.1 Precipitation of particles

The present study is focused mainly on grain growth. Precipitation behaviour associated with different types of particles, therefore, will be discussed very briefly and only in context of the grain growth. Although, additional and detailed investigations of chemical and phase composition of the particles are necessary, their spatial distribution and volume fraction will be essential to discuss the precipitation behaviour in some detail.

In order to ascertain macro-scale features of grain growth, the summarized macro-scale distribution of the particles in the as-FSWed state (Table 1) shall be considered. The minimal $\sum S$ value in the border parts of SZ (Top zone and Bottom) can be rationalized in a general way by the time-temperature predictions as follows. The border parts of SZ would experience a faster quenching during the cooling cycle of the weld because of convection in the Top zone and of heat sinking into a back plate in the Bottom. Correspondingly, the cooling rate in the central part of SZ would be lowest. The faster quenching implies shorter time for re-precipitation of particles from solid-solution. Therefore, the minimal $\sum S$ value in Top zone and Bottom might be attributed to a faster cooling rate. The cause of the decrease in $\sum S$ value from AS to RS is less clear but it may be related to temperature heterogeneity in SZ during FSW. For example, Cho *et al*[14] have found experimentally that temperature in AS is higher than in RS. Higher temperature (under the same other conditions) shall lead to faster diffusion of constituent atoms as well as longer cooling time and, therefore, to more complete particles precipitation. Thus, FSW-induced macro-scale heterogeneity in particles distribution within SZ is thought to be not incidental but inherent to FSW treatment.

To consider the grain growth behavior in meso-scale, it is essential to look into alignment of the different types of particles along the flow patterns. This flow pattern is a feature of the as-FSWed state and it does not disappear during precipitation of new particles at the temperatures of 250°C and 400 to 450°C (see Fig. 7(f) and Fig. 9(c)). Minor effect of the heat treatments on the particles distribution heterogeneity is thought be caused by the following reason : As it was stated above, the as-FSWed structure consisted of alternating bands of fine and coarse grains aligned with the flow patterns (Fig. 4). Precipitation of particles at grain boundaries would be more preferential in bands of fine grains because of higher fraction of grain boundaries. Thus, alignment of the precipitated particles with flow patterns is thought be attributed to banded microstructure inherent to the as-FSWed state.

4.2 Grain growth

One of the most significant features among all structures evolved due to the heat treatments in the temperature range of

250-450°C is an enormous difference between sizes of individual coexisting grains (Fig. 7(a) to (d) and Fig. 9(a), (b) and (d)). This fact indicates that grain growth occurred discontinuously, with certain grains growing preferentially and consuming the surrounding finer grains. This process is well described as *abnormal grain growth* (secondary recrystallization). Hereafter, the common features of this process are considered and its possible reasons are discussed.

4.2.1 Macro-scale analysis

A common macro-scale feature of all above-mentioned states is the inequality of grain growth in different parts of SZ. It must be caused, firstly, by the variation of thermal stability (in the temperature range of 250–350°C (see Fig. 6) and, secondly, by the variations of both shape and size of the abnormal coarse grains (in the temperature range of 400–450°C (see Fig. 8). Similar trends have been observed by many authors.[2,3,5,6]

As well known, thermal stability of alloys containing second-phase particles (including ZK60) depends on a pinning stress of secondary particles[e.g.10] and, thereby, on particles surface area. In our case, specific surface area, ($\sum S$ value) changed significantly across SZ in the as-FSWed state (Table 1). In this regard, the variation of thermal stability across SZ can be attributed to the macro-scale heterogeneity of particles distribution. Indeed, grain growth was initiated, first of all, in the periphery region of SZ, i.e., Top Zone and Bottom (Fig. 6); it matches well with a reduced $\sum S$ value in these regions (Table 1). Grains grew faster in RS than in AS (Fig. 6); it matches also for the decrease in $\sum S$ value from AS to RS (Table 1). The minimal thermal stability was observed in Top RS and Top Center (200°C – Fig. 6(a)) and the maximum one – in Central zone and AS (300°C – Fig. 6(b) and (c)); It correlates well with minimal and maximum $\sum S$ values in these regions correspondingly.

The variation in grain size across SZ (Fig. 8) can be also explained in terms of macro-scale heterogeneity in spatial distribution of particles. A lower $\sum S$ value would lead to the preferential growth of many grains simultaneously, resulting in a relatively fine and uniform final structure. Conversely, a higher $\sum S$ value can activate catastrophic growth of fewer grains, eventually leading to coarser and inhomogeneous structure. Indeed, minimal grain size observed in Top zone and Bottom, maximum grain size in Central zone and AS, and the decrease in grain size from AS to RS (Fig. 8) correspond well with the variation in $\sum S$ value in the as-FSWed state (Table 1).

Thus, macro-scale heterogeneity in spatial distribution of secondary particles, inherent to the as-FSWed state, correlates well with the variations of both thermal stability and grain sizes across SZ.

4.2.2 Meso-scale analysis

One of the most significant features of meso-scale structure is the alignment of growing grains with the flow patterns. The similar tendency has been observed in many studies.[2–4,6] Taking into account that different types of particles were also aligned with the flow patterns (Fig. 7(f) and 9(c)), it can be assumed that the grain growth depended also on meso-scale heterogeneity in spatial distribution of the particles. For clear understanding of this phenomenon, the sequence of the grain growth is discussed in some detail here.

As it follows from the comparison of Fig. 4(d) and Fig. 9(b), the grain size in the remainder structure, survived from annealing, is close to the grain size corresponding to that in the fine-grain bands of the as-FSWed structure. Stagnation of grain growth in this microstructure might be attributed to higher density of fine particles (Fig. 9(d)). On the other hand, rapidly growing grains were observed in coarse-grained bands of the as-FSWed structure (Fig. 7(d)). Summarizing all above-mentioned facts, we can conclude that *grain growth was initiated in the coarse-grained bands of the as-FSWed structure*. It is important to note that the fraction of boundaries in these bands is smaller than the one in the fine-grained bands; thus, driving force for grain growth is probably lower in the bands. Hence, higher boundaries mobility in the coarse-grained bands, caused by a lower particles pinning pressure, would be the primary factor that controls grain growth in the present case.

Of particular interest is the observation that at the beginning stage of grain growth the average size of growing grains is approximately the same as that within the isolated bands (Fig. 7(e)). Hence, we can conclude that, in scale of these bands, *onset of grain growth was rather normal (continuous) than abnormal*. On the other hand, in scale of whole microstructure, grain growth begins within isolated bands of grains only and a number of surrounding grains are kept unchanged (Fig. 7(e)); this grain growth behavior is obviously abnormal (discontinuous).

Advanced stage of grain growth was characterized by the following two features. Firstly, the increase in grain size was accompanied by grain shape change– grains were elongated in the direction of the flow patterns (Fig. 7(d)). Secondly, sizes of growing grains became very different (Fig. 7(d)). These facts can be explained as follows: Grain growth is normal before growing grains reach the border of the particle rich layers (fine-grained bands). Grain boundary migration in particle poor layers (coarse-grained bands) is evidently faster than in the particle rich layer. At this point, grain growth becomes directional and, in such a way, the shape of growing grain gradually resembles the flow patterns. Correspondingly, meso-scale variations in the particle density allow some grains to grow preferentially and, therefore, lead to abnormal grains growth.

Thus, the abnormality and selectivity of grain growth would be attributed to meso-scale heterogeneity in spatial distribution of particles, i.e. the existence of the banded structure in the as-FSWed state. However, the shape of some grains was equiaxial in Top RS and Top Center (Fig. 8(b)), while it was irregular in Central zone (Fig. 8(a)). Hereafter we discuss these cases in some detail.

As stated in section 3.1, plastic flow in Top RS and Top Center during FSW was quite complex. We suggest that additional mixing of material in these regions can result in more homogeneous distribution of the particles, which eventually affect the grain growth behavior. In addition, the minimal $\sum S$ value corresponding to these regions (Table 1) can promote a greater number of simultaneously growing grains and, consequently, lead to local formation of more uniform structure.

Central zone in the as-FSWed state was characterized by the most homogeneous microstructure (Fig. 3(a)), i.e., large

fraction of high-angle boundaries (Fig. 3(b)), uniform distribution of the particles and high $\sum S$ value (see Table 1). According to Humphreys,[9,10] similar structures are highly stable. In this regard, transformation of structure in Central zone can be attributed not to own grain growth but to expansion of abnormal growing grains from adjacent regions, most likely from Top zone (see Fig. 6(c)). The irregular shape of grains in Central zone (Fig. 8(a)) can be caused by homogeneous distribution of the particles.

4.2.3 Micro-scale analysis

Substructure within the abnormal coarse grains (Fig. 7(a) and (c), Fig. 9(a) and (b)) and jagged nature of their boundaries (Fig. 7(a)) are common micro-scale features of the developed structures. The similar peculiarities have been found also in many studies.[2,3,5] It should be emphasized that these features are generally inherent to secondary recrystallization[e.g.15].

The ragged nature of the growth front of the abnormal coarse grains suggests that its progress was strongly influenced by local variations of the structure. Thus, in contrast to meso-scale, grain boundary migration in micro-scale was rather chaotic.

The abnormal coarse grains were normally surrounded by a number of much smaller grains (Fig. 7(a)). Probably, the amount of defects in these grains (dislocation density, internal stress/strain and so on) is different from each other. Consequently, driving force for the migration of a boundary of the abnormal coarse grain would vary along the growth front. On the other hand, grain boundary mobility would also be locally different due to heterogeneous particles distribution. Therefore, the very complex shape of the abnormal coarse grains (Fig. 7(b)) is thought to be caused by local variations of driving force for grain boundary migration.

Remnant microstructure, survived during the abnormal grain growth (Fig. 9(c)), can also be attributed to local heterogeneity in boundaries migration. Owing to local high particles density and/or low amount of defects, some groups of original grains can maintain longer time as compared to their neighbors and, in such a way, they can be found either between two abnormal coarse grains (Fig. 9(d)) or even within them (Fig. 9(b)). The subsequent evolution of the microstructure can gradually reduce a number of grains in these 'islands' (Fig. 7(a), selected region) until their full disappearance. On the other hand, these small grains can also grow; as a result, slightly grown grains can be found within the much coarse ones (Fig. 9(a)).

4.2.4 Precautions of abnormal grain growth

In our experiment, the abnormal grain growth occurred even under concurrent precipitation of second-phase particles in the temperature range of 400 to 450°C (Fig. 8 and 9). It implies that, in spite of common opinions,[2–6] a main reason of secondary recrystallization in our case would not be dissolution of the particles. As we discussed above, a key factor that controlled the grain growth behaviour would be a heterogeneous particle density. Hence, to avoid abnormal grain growth, an obvious solution can be to improve homogeneity of particle spatial distribution through artificial aging of FSWed structure, as an example.

An alternative approach would be optimisation of FSW parameters. According to recent conception,[16] FSWed structure is directly dependent on N/V value i.e., tool advance per revolution. In this regard, there is an opportunity to manipulate FSW parameters in order to improve structure homogeneity. For example, performing FSW at a higher N/V value will result in a higher heat input and can eventually lead to more homogeneous structure formation, including secondary particles. On the other hand, the increase of N/V ratio will decrease flow patterns spacing.[13] Since variation in the local particles density is directly correlated with the flow patters, this also can improve homogeneity of particles distribution.

However, when the N/V value was much higher, the possibility of the formation of weld defects would increase. We should, therefore, select proper N/V value.

5. Conclusions

Grain growth behaviors in FSWed ZK60 magnesium alloy were investigated and the following conclusions were obtained:

(1) The grain growth behavior was characterized by the following features:
   (a) Different thermal stability was observed in different regions of SZ. The minimal thermal stability corresponded to Top RS region at 200°C, and the maximal one to Central zone at 300°C.
   (b) Grain growth behavior was abnormal;
   (c) Grain growth was directional and the shape of abnormal coarse grains resembled flow patterns inherent to FSWed structure;
   (d) In different regions of SZ, different average sizes of the developed abnormal coarse grains were observed. Average grain size in the periphery region of SZ (Top zone and Bottom) was significantly smaller than that in its central part; the grain size gradually decreased from AS to RS;

(2) All peculiarities of the grain growth can be explained in terms of heterogeneity of spatial distribution of second-phase particles inherent to the as-FSWed state. Abnormality and selectivity of grain growth seemed to be attributed to meso-scale variation in local particles density. Variations of both thermal stability and sizes of abnormal coarse grains across SZ seemed to be attributed to macro-scale heterogeneity in spatial distribution of secondary particles.

Acknowledgements

Authors would like to thank Dr. Goloborodko for his help in EBSD analysis and Mr. T. Shibata and Ms. J. Aihara for their help in EDX analysis at Oarai Research Institute (JAEA). One of the authors (S. Mironov) would like to thank Dr. T. Ito, Mr. X. Yun and Mr. T. Sakuma for their help in realization of experiments. We also greatly acknowledge the Light Metal Educational Foundation for their financial support.

REFERENCES

1) W. M. Thomas: Friction stir butt welding, Int. Patent No PCT/GB92/

02203 (1991), and US Patent No. 5, 460, 317 (1995).
2) Kh. A. A. Hassan, A. F. Norman, D. A. Price and P. B. Prangnell: Acta Mater. **51** (2003) 1923–1936.
3) M. M. Attallah and H. G. Salem: Mat. Sci. and Eng. **391** (2005) 51–59.
4) I. Charit, R. S. Mishra, M. W. Mahoney: Scripta Mat. **47** (2002) 631–636.
5) A. Goloborodko, T. Ito, X. Yun, Y. Motohashi and G. Itoh: Mater. Trans. (JIM) **45** (2004) 2503–2508.
6) I. Charit and R. S. Mishra: Acta Mat. **15** (2005) 4211–4223.
7) Ø. Friggard, Ø. Grong and O. T. Midling: Metall. Trans. A, **32A**, (2001) 1189–1200.
8) Y. S. Sato, H. Watanabe, S. H. C. Park and H. Kokawa: Proc. 5th Int. FSW Sympo., Metz, France, (2004), CD-ROM.
9) F. J. Humphreys: Acta Mater. **45** (1997) 4231–4240.
10) F.J. Humphreys: Acta Mater. **45** (1997) 5031–5039.
11) S. A. Saltykov: *Stereometrical Metallography*, (Metallurgy, Moscow, 1976) pp. 148–156 (in Russian).
12) Y. Li, L. E. Murr and J. C. McClure: Mat. Sci. and Eng. **A271** (1999) 213–223.
13) K. N. Krishnan: Mat. Sci. and Eng. **A327** (2002) 246–251.
14) J.-H. Cho, D. E. Boyce and P. R. Dawson: Mat. Sci. and Eng. **A 398** (2005) 146–163.
15) Y. Ushigami, T. Kubota and N. Takahashi: ISIJ International **38** (1998) 553–558.
16) R. S. Mishra and Z. Y. Ma: Mat. Sci. and Eng. R **50** (2005) 1–78.